ISSN 2079-1704. Хімія, фізика та технологія поверхні. 2026. Т. 17. № 1. С. 83-92

UDC 539.261 doi: 10.15407/hftp17.01.083

Y.O. Kovalskyi [1], V.A. Karpyna [1], L.A. Myroniuk [1], O.I. Olifan [1], S.F. Korichev [1], I.M. Danylenko [2], S.P. Starik [3], V.V. Strelchuk [2], A.I. Ievtushenko [1]

PROPERTIES OF ZnO-Zn CONGLOMERATES GROWN ON UNPOLISHED Si SUBSTRATE BY CARBOTHERMAL REDUCTION UNDER RAPID SOLAR EVAPORATION

[1] Frantsevich Institute for Problems of Materials Science of National Academy of Sciences of Ukraine
3 Omeljana Pritsaka Str., Kyiv, 03142, Ukraine, E-mail: y.kovalskyi@ipms.kyiv.ua
[2] V. Lashkaryov Institute of Semiconductor Physics of National Academy of Sciences of Ukraine
45 Nauky Aven., Kyiv, 03028, Ukraine
[3] V. Bakul Institute for Superhard Materials of National Academy of Sciences of Ukraine
2 Avtozavodskaya Str., Kyiv, 04074, Ukraine

This paper presents the results of a study of ZnO-Zn conglomerates synthesised on unpolished silicon (Si) substrates by the rapid solar evaporation method of ZnO/C precursors with mass ratios of 2:1 and 1:3. The obtained samples were analysed using X-ray structural analysis, which confirmed the formation of a wurtzite-type ZnO crystalline phase and metallic Zn. Photoluminescence spectra revealed two characteristic peaks: a near band edge emission at ~380 nm, caused by exciton recombination, and an intense green band at ~522 nm associated with oxygen vacancies. Raman spectroscopy revealed a shift in the E_2 (high) mode, which characterizes the oscillation of the oxygen sublattice, from 437 to 427 cm^{-1}, indicating an increase in the lattice period because of elastic stresses in the crystallites. Energy dispersive analysis showed the distribution of grown ZnO and Zn conglomerates. The photocatalytic properties, which were studied by degrading the model dye methyl orange under UV irradiation, showed better values in the case of ZnO-Zn conglomerate synthesis at a precursor concentration of ZnO/C as 1:3. The results obtained demonstrate the promise of using concentrated solar radiation for the synthesis and creation of materials with the desired properties using environmentally friendly, energy-independent technologies.

***Keywords**: ZnO-Zn conglomerates, carbothermal reduction, morphology, photoluminescence, photocatalysis*

INTRODUCTION

Materials based on ZnO are one of the most researched for photocatalytic applications because they are low-cost to manufacture, non-toxic, chemically and radiation stable, readily available, have high UV absorption, and a wide variety of synthesis methods [1–4]. However, the use of pure ZnO as a photocatalyst is limited by the high recombination rate of photogenerated electron-hole pairs and insufficient photosensitivity in the visible range [5]. Last years, scientists have investigated several strategies to improve the photocatalytic performance of ZnO-based photocatalysts, such as fabricating different hierarchical nanostructured morphologies, surface modification with organic compounds, doping with foreign ions, noble metal deposition on the oxide surface, the creation of heterostructures with other semiconductors, and the control of point defects, *etc*. [6–8]. It has been suggested that such an approach in the modification of ZnO can significantly improve the charge separation, facilitate the generation of reactive oxygenated free radicals, and, thus, increase its interaction with the pollutant molecules.

Various ZnO morphologies, such as nanocrystals, nanorods, nanowires, nanotubes, nanoneedles, nanoribbons, and nanosheets, are being actively researched to create effective photocatalysts [9]. The synthesis of ZnO nanostructures is carried out using both physical and chemical methods, in particular: thermal evaporation [10], chemical vapour phase deposition (CVD) [11], vapour phase epitaxy [12], molecular beam epitaxy [13], reactive magnetron sputtering [14], hydrothermal synthesis [15], sol-gel techniques [16], galvanoplasty [17] and pyrolysis [18]. Most of these methods require high-temperature conditions, complex vacuum equipment or lengthy synthesis, which limits their widespread applications.

One of the approaches to improving its photocatalytic properties is to combine ZnO with

© Y.O. Kovalskyi, V.A. Karpyna, L.A. Myroniuk, O.I. Olifan, S.F. Korichev, I.M. Danylenko, S.P. Starik, V.V. Strelchuk, A.I. Ievtushenko, 2026

carbon materials, in particular graphene, graphene oxide (GO), carbon nanotubes (CNT) and activated carbon [19–21]. The carbothermal reduction reaction, which uses ZnO and C powders as initial precursors, can be used to synthesise ZnO in the form of nanostructures [22]. Non-stoichiometry of components in the mixture of ZnO/C precursors may lead to carbon residue coating the grown ZnO nanostructures. Otherwise, in Ref. [23] was proposed two-step water splitting cycles using Zn–ZnO redox pair for the solar production of hydrogen. Hence, it is useful to study ZnO-Zn samples grown using carbothermal reduction for possible application in photocatalytic processes.

Previously, we proposed a new rapid ("explosive") solar evaporation (RSE) method [24] for growing ZnO films and nanostructures, which uses concentrated solar radiation to evaporate zinc acetylacetonate or mixtures of ZnO/C powders precursors to realise the MOCVD growth process or carbothermal reduction deposition, respectively.

Our work is devoted to investigating the effect of the mass ratio of ZnO and C powders in proportions (2:1 and 1:3) on the structure, surface morphology, elemental distribution, Raman scattering, photoluminescence and photocatalytic activity of ZnO–Zn conglomerates grown on unpolished Si substrates by carbothermal reduction in RSE method.

RESEARCH METHODS AND OBJECTS

ZnO-Zn conglomerates were obtained by carbothermal reduction [25] on unpolished Si substrates (10×10 mm^2) using RSE method and carbothermal reduction reaction. A solar concentrator based on a converted army floodlight located at Frantsevich Institute for Problems of Materials Science, National Academy of Sciences of Ukraine (Fig. 1), was used to evaporate the ZnO/C precursors with various proportions (2:1 and 1:3). The solar concentrator (Fig. 1) contains a mirror with a diameter of 100 cm, which ensures that temperatures of about 1000 °C are reached at the focus of the solar radiation when the blinds are fully open (angle 90°).

Fig. 1. Solar concentrator (Frantsevich Institute for Problems of Materials Science, NAS of Ukraine, Kyiv, Ukraine)

During the synthesis of samples, a mixture of ZnO and C powders with a total mass of 1 g was used in proportions of ZnO/C as 2:1 (for the growth of samples A and B) and ZnO/C as 1:3 (for the growth of samples C and D). Unpolished Si substrates were placed in a quartz tube at different

distances from 4 to 10 cm from the evaporation zone of ZnO/C precursor, where solar energy was focused. The other end of the quartz tube remained open, providing air access and removal of reaction products. The deposition time was about 2 minutes. The geometry of the experiment and the designation of the samples are shown in Fig. 2.

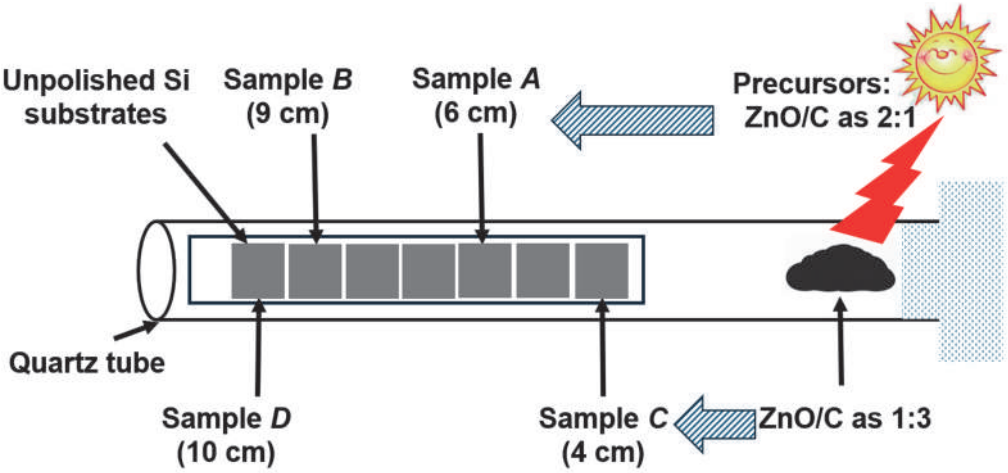

Fig. 2. Schematic illustration of the process for carbothermal reduction in the rapid solar evaporation method and designation of ZnO-Zn samples

ZnO is reduced by C at temperatures above 900 °C. Since the melting point of Zn is 419 °C, Zn can exist in the liquid phase at a certain vapour pressure in the form of liquid droplets, which can act as nucleation and growth centres for ZnO nanocrystals. Zn vapours in the carbothermal reduction process are actively oxidised to a stable ZnO phase [22, 25]. Thus, ZnO nanocrystals should condense in areas of the quartz tube outside the solar focus, *i.e.* at temperatures below 900 °C. The structure, morphology, and elemental composition of these nanostructures are determined by the temperature, vapour pressure above the substrate, the nature of the substrate and the composition of ZnO/C precursor.

To study the crystal structure of ZnO, we used X-ray diffraction with a DRON-4 diffractometer with CuK_α radiation ($\lambda = 0.1541$ nm). Using a ZEISS EVO 50 XVP scanning electron microscope, high-resolution images of the grown conglomerates were obtained. The elemental composition of the samples was determined using an Ultim Max 100 energy dispersive X-ray spectrometer (Oxford Instruments plc, UK). The photoluminescence (PL) spectra were measured at room temperature using a He-Cd laser excitation (325 nm) on a Horiba Jobin-Yvon T64000 spectrophotometer (France).

Raman scattering spectra were recorded on a Horiba Jobin-Yvon T64000 spectrometer equipped with a CCD detector at room temperature in backscattering geometry. The radiation from a laser (532 nm) was focused on the sample using an Olympus BX 41 microscope and used to study combination scattering under non-resonant conditions. The diameter of the analysed spot was 1 μm, and the spectral resolution was 1 cm^{-1}.

The transmission spectra of aqueous solutions of methyl orange (MO) were obtained using a Shimadzu UV2600i double-beam UV spectrophotometer.

RESULTS AND DISCUSSION

X-ray diffraction patterns of all grown samples (Fig. 3), deposited at different ZnO/C precursor ratios and different precursor-substrate distances, indicate the formation of ZnO and Zn phases. Thus, according to the JCPDS No. 87-0713 diffraction pattern, the peak position at $2\theta \approx 36.25°$ corresponds to the reflection of X-rays from the (101) planes of hexagonal ZnO. The positions of the other peaks coincide with the hexagonal Zn phase (JCPDS No. 36-1451). The most intense among them is the (101) reflection at $2\theta \approx 43.22°$.

By approximating the X-ray peaks using the Gaussian function in the Origin software, their positions and full width at half maximum (FWHM) were determined.

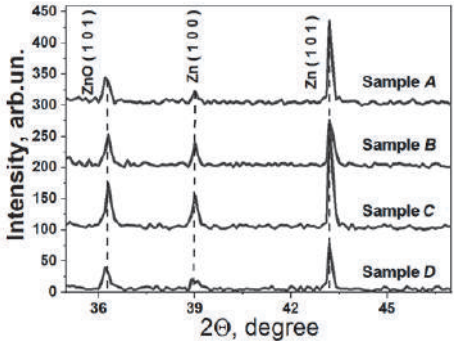

Fig. 3. X-ray diffraction patterns of ZnO-Zn conglomerates

The Scherrer equation was used to determine the size of crystallites (D) [26]:

$$D = \frac{k\lambda}{\beta \cos \theta}, \quad (1)$$

where k is the shape factor (approximately 0.93), λ is the X-ray wavelength (0.1541 nm), β and θ denote the full width at half maximum (FWHM) and the diffraction angle for plane (101), respectively. The results of the crystallite size calculations are given in Table 1.

The interplane distance (d) was calculated using the Bragg formula [27]:

$$n\lambda = 2d\sin\theta, \quad (2)$$

where $n = 1$ is the diffraction order, $\lambda = 0.1541$ nm is the wavelength of CuK_α radiation, and θ is half the angle 2θ determined from the experimental data.

The obtained values for the most intense XRD peaks of ZnO (101) and Zn (101), the size of crystallites (D) and the interplane distance (d) are given in Table 1.

Table 1. Results of X-ray diffraction analysis of ZnO-Zn conglomerates grown on Si substrate with ratios ZnO/C as 2:1 and ZnO/C as 1:3

Sample	ZnO crystallites				Zn crystallites			
	XRD peak (101), deg	**FWHM of (101) peak, deg**	***D*, nm**	***d*, nm**	**XRD peak (101), deg**	**FWHM of (101) peak, deg**	***D*, nm**	***d*, nm**
	ZnO/C as 2:1							
A	36.24	0.25	33	0.2474	43.22	0.11	73	0.2093
B	36.29	0.19	43	0.2471	43.23	0.15	54	0.2092
	ZnO/C as 1:3							
C	36.31	0.17	49	0.2470	43.23	0,11	73	0.2092
D	36.23	0.19	43	0.2475	43.22	0,13	61	0.2093

As can be seen from Table 1, at a ZnO/C precursor ratio of 2:1, the size of crystallites (D) for ZnO are 33–43 nm, and for Zn are 54–73 nm, respectively. With an increase in the carbon concentration in powder mixture ZnO/C as 1:3, D increase to 43–49 nm for ZnO and 61–73 nm for Zn comparison with the samples deposited from ZnO/C 2:1. This indicates more favorable crystallization conditions for both ZnO and Zn phases in an environment with a higher carbon content, which probably contributes to the formation of larger crystallites.

SCANNING ELECTRON MICROSCOPY

SEM images of ZnO-Zn conglomerates deposited on unpolished Si substrates are shown in Fig. 4. The grown ZnO-Zn conglomerates practically uniformly cover the surface of the Si substrate (Fig. 4 *b*). It has been found that the surface of the samples consists of ZnO conglomerates with sizes in the range of 40–60 nm and separate Zn microcrystals in the form of spheres with diameters in the range of 500–3500 nm.

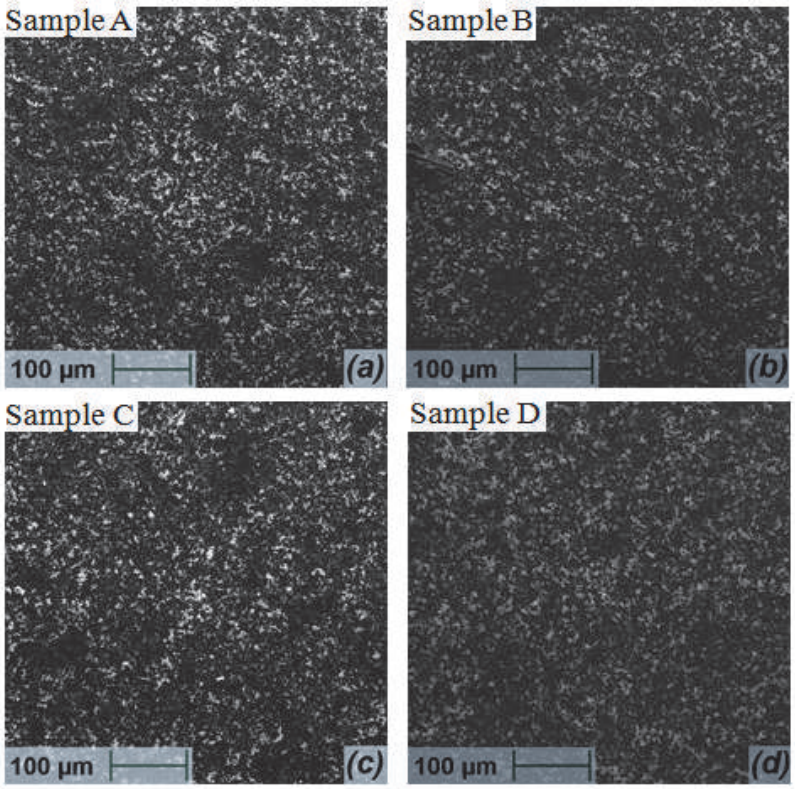

Fig. 4. SEM images of ZnO-Zn conglomerates grown on unpolished Si substrates from ZnO/C as 2:1 (*a*, *b*) and ZnO/C as 1:3 (*c*, *d*) ratios

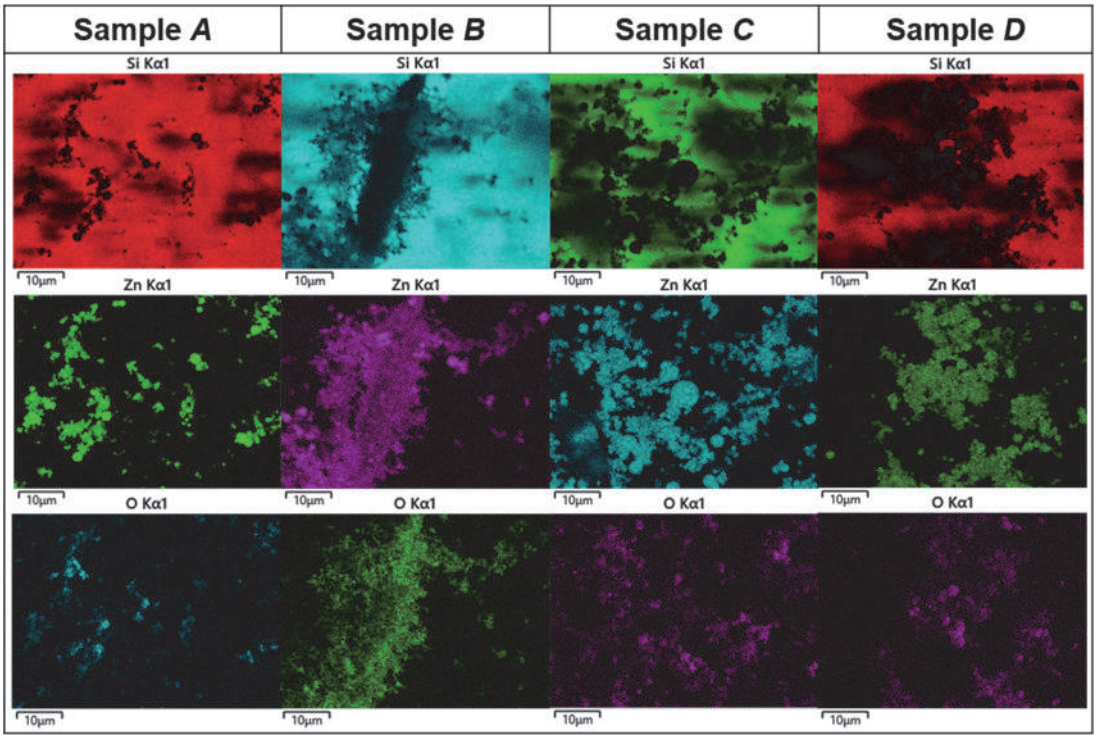

Fig. 5. Elemental distribution of Si, Zn and O for samples synthesized at mass ratios of precursors ZnO/C as 2:1 and ZnO/C as 1:3

To determine the elemental composition and distribution of elements in the plane of the synthesized samples, energy dispersive X-ray (EDX) analysis was performed with the construction of distribution maps of elements – silicon (Si Kα), zinc (Zn Kα) and oxygen (O Kα) (Fig. 5). EDX analysis confirms the presence of Zn and O on the Si substrate. Detailed analysis of the elemental distribution of the samples determined that ZnO was grown in the form of crystallites and Zn in the form of spheres (Fig. 5).

Thus, the combination of SEM and EDX analysis demonstrates that an increase in the carbon content of the precursor contributes to the formation of a more ordered morphology and the growth of ZnO-Zn conglomerates. This confirms the possibility of effective control of the Zn phase content in ZnO-Zn conglomerates by varying the ZnO/C ratio.

PHOTOLUMINESCENCE

Fig. 6 shows the photoluminescence (PL) spectra of ZnO-Zn conglomerates (measured at room temperature) grown on a Si substrate with a ratio of ZnO/C as 2:1 and ZnO/C as 1:3. It was noted that all samples have two characteristic bands at 380–385 and 522–526 nm.

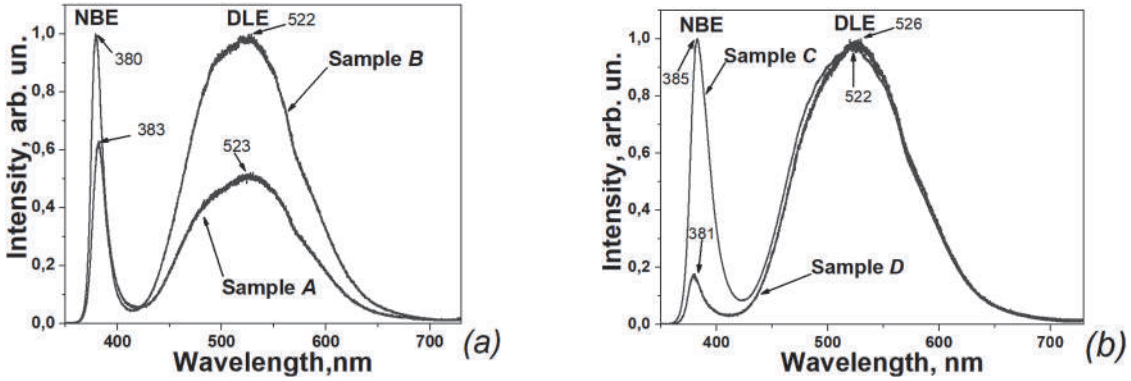

Fig. 6. Normalized photoluminescence spectra of ZnO-Zn conglomerates grown on unpolished Si substrate with ratios of ZnO/C as 2:1 (*a*) and ZnO/C as 1:3 (*b*)

The emission peak at about 380 nm is attributed to near-band edge emission (NBE) [28] and the green emission peak at about 522 nm is caused by oxygen vacancies which are formed at the deep donor level in the bandgap of the material [29]. Changing the ZnO/C ratio in precursor mixtures and the distance precursor-substrate leads to a change in the ratio of integrated intensities INBE/IDLE for samples A, B, C, and D as 0.13, 0.06, 0.13, and 0.01, respectively (Fig. 6). This indicates the worst photoluminescence in sample D, where Zn spheres are dominated.

RAMAN SPECTRA

The typical nonresonant Raman spectra of the ZnO-Zn conglomeration excited at room temperature by a 532.0 nm laser line are shown in Fig. 7. The Raman spectra of the grown samples show characteristic Raman bands of polycrystalline wurtzite-type ZnO [30, 31]. We have observed common phonon Raman modes of ZnO centered at ~98, ~328, 427–435, and ~581 cm^{-1} corresponding E_2^{Low}, $E_2^{High} - E_2^{Low}$, E_2^{High}, and quasi-A_1^{LO} modes, respectively. Variations in Raman position modes are caused by changing structural ZnO defects, and by possible interaction of ZnO with carbon components.

PHOTOCALYTIC STUDY

The efficiency of photodegradation of the model dye methyl orange (MO) by ZnO-Zn conglomerates immobilized on the solid surface of a silicon substrate was evaluated by the decrease in the concentration of the dye in the solution. To study the photocatalytic activity of the silicon substrate, coated with ZnO-Zn conglomerates, with an area of about 1×1 cm^2, it was immersed in an aqueous solution of MO. Before irradiation, the samples were kept in the dark for 12 hours to achieve adsorption-desorption equilibrium. The initial MO concentration was selected as 10 mg/l as optimal [32]. The samples were then irradiated with a

200 W mercury UV lamp for 1, 3 and 6 hours, respectively. The change in dye concentration in each solution was monitored by measuring the transmittance of the solution at 465 nm. The transmittance spectra of MO aqueous solutions were obtained using a Shimadzu UV2600i dual-beam UV spectrophotometer. The photodegradation efficiency (DE) of the MO dye was calculated using formula (3) [19]:

$$DE(\%) = \frac{C_0 - C_t}{C_0} \times 100\%, \quad (3)$$

where C_0 is the initial concentration of the dye, C_t is the concentration of the dye at time t, after irradiation with a mercury lamp, respectively. The results of the calculations are shown in Fig. 8.

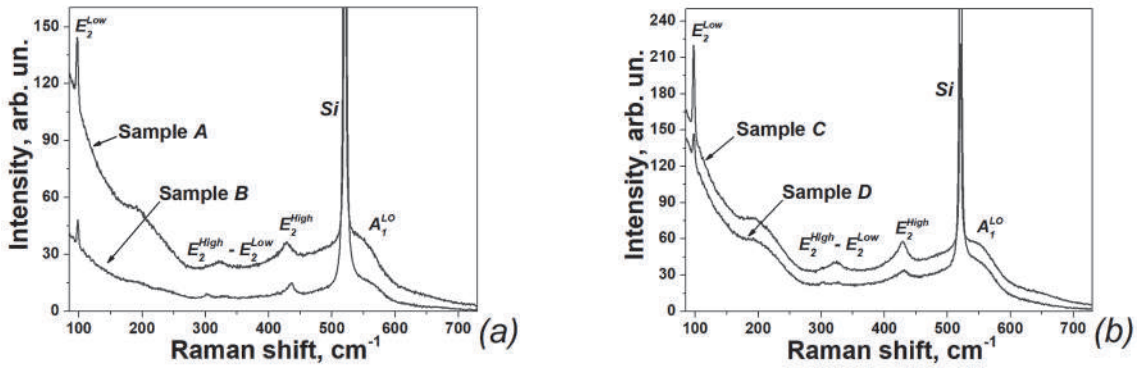

Fig. 7. Raman spectra of the grown ZnO-Zn conglomerates obtained by evaporation of precursors ZnO/C = 2:1 and ZnO/C = 1:3

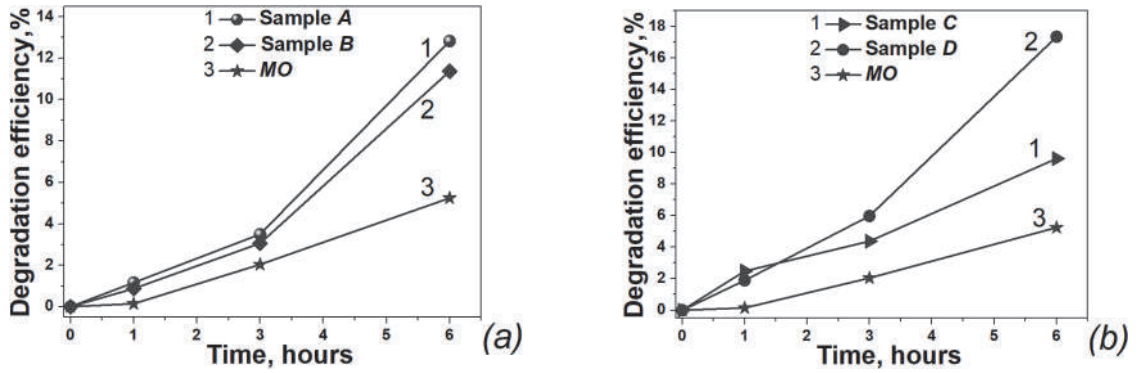

Fig. 8. Photocatalytic efficiency of ZnO-Zn conglomerates grown on unpolished Si substrate with ZnO/C ratios of 2:1 (*a*) and 1:3 (*b*)

The samples obtained with a ZnO/C as 2:1 component ratio demonstrated a photocatalytic efficiency of 11–13 % (Fig. 8 *a*) for the decomposition of the MO dye, while this indicator for ZnO/C = 1:3 samples was about 9–17 % (Fig. 8 *b*). The best photocatalytic efficiency is demonstrated by sample D, which has the worst photoluminescence, suggesting a significant influence of oxygen vacancies on photocatalytic efficiency for ZnO-Zn samples [33].

CONCLUSIONS

ZnO-Zn nanostructured conglomerates were grown by carbothermal reduction on unpolished Si substrates by RSE method using mixtures ZnO and C as initial precursors. XRD patterns, scanning electron microscopy and energy dispersive X-ray (EDX) analysis demonstrate that the surface morphology of samples is formed by ZnO conglomerates with sizes in the range of 40–60 nm and separate Zn microcrystals in the form of spheres with diameters in the range of 500–3500 nm. All ZnO-Zn samples have the green emission peak at about 522 nm (2.38 eV), which is caused by oxygen vacancies formed at the deep donor level in the bandgap of the material, and phonon Raman modes of ZnO centered at ~98, ~328, 427–435, and ~581 cm^{-1}

corresponding E_2^{Low}, E_2^{High}–E_2^{Low}, E_2^{High}, and quasi - A_1^{LO} modes, respectively. The best photodegradation of methyl orange dye was observed for the ZnO-Zn sample, which has the worst photoluminescence, suggesting a significant influence of oxygen vacancies on the efficiency of photocatalysis processes in ZnO. Optimization of the structure and morphology of ZnO-Zn conglomerates is necessary to increase their photocatalytic activity.

Властивості конгломератів ZnO-Zn, вирощених на неполірованій підкладці Si методом карботермічного відновлення при швидкому сонячному випаровуванні

Ю.О. Ковальський, В.А. Карпина, Л.А. Миронюк, О.І. Оліфан, С.Ф. Корічєв, І.М. Даниленко, С.П. Старик, В.В. Стрельчук, А.І. Євтушенко

Інститут проблем матеріалознавства ім. І.М. Францевича Національної академії наук України
вул. Омеляна Пріцака, 3, Київ, 03142, Україна, y.kovalskyi@ipms.kyiv.ua
Інститут фізики напівпровідників ім. В.Є. Лашкарьова Національної академії наук України
пр. Науки, 41, Київ, 03028, Україна
Інститут надтвердих матеріалів ім. В.М. Бакуля Національної академії наук України
вул. Автозаводська, 2, Київ, 04074, Україна

У статті представлені результати дослідження конгломератів ZnO-Zn, синтезованих на неполірованих підкладках кремнію (Si) методом швидкого сонячного випаровування прекурсорів ZnO/C з масовим співвідношенням 2:1 та 1:3. Отримані зразки були проаналізовані за допомогою рентгенівського структурного аналізу, який підтвердив утворення кристалічної фази ZnO типу вюртциту та металічного Zn. Спектри фотолюмінесценції виявили два характерні піки: випромінювання поблизу краю смуги при ~380 нм, спричинене рекомбінацією екситонів, та інтенсивну зелену смугу при ~522 нм, пов'язану з вакансіями кисню. Раманівська спектроскопія виявила зсув в режимі E_2 (high), який характеризує коливання підґратки кисню, з 437 до 427 $см^{-1}$, що вказує на збільшення періоду ґратки в результаті пружних напружень в кристалітах. Енергодисперсійний аналіз показав розподіл вирощених конгломератів ZnO і Zn. Фотокаталітичні властивості, які вивчалися шляхом розкладання модельного барвника метилового оранжового під дією УФ-випромінювання, показали кращі значення у випадку синтезу конгломератів ZnO-Zn при концентрації прекурсорів ZnO/C як 1:3. Отримані результати демонструють перспективність використання концентрованого сонячного випромінювання для синтеза та створення матеріалів з бажаними властивостями за допомогою екологічно чистих, енергонезалежних технологій.

***Ключові слова**: ZnO-Zn конгломерати, карботермічне відновлення, морфологія, фотолюмінесценція, фотокаталіз*

REFERENCES

1. Karpyna V.A., Myroniuk L.A., Myroniuk D.V., Bugaiova M.E., Petrosian L.I., Bykov O.I., Olifan O.I., Strelchuk V.V., Kolomys O.F., Romanyuk V.R., Naumenko K.S., Artiukh L.O., Povnitsa O.Y., Zahorodnia S.D., Ievtushenko A.I. Photocatalysis and optical properties of ZnO nanostructures grown by MOCVD on Si, Au/Si and Ag/Si wafers. *Himia, Fizika ta Tehnologia Poverhni.* 2023. **14**(1): 83.
2. Baibara O.E., Radchenko M.V., Karpyna V.A., Ievtushenko A.I. A Review of the Some Aspects for the Development of ZnO Based Photocatalysts for a Variety of Applications. *Phys. Chem. Solid State*. 2021. **22**(3): 585.
3. Myroniuk D.V., Ievtushenko A.I., Lashkarev G.V., Maslyuk V.T., Timofeeva I.I., Baturin V.A., Karpenko O.Y., Kuznetsov V.M., Dranchuk M.V. Effect of electron irradiation on transparent conductive films ZnO:Al deposited at different power sputtering. *Semicond. Phys. Quantum Electron. Optoelectron.* 2015. **18**(3): 286.

4. Ievtushenko A., Karpyna V., Myroniuk L., Myroniuk D., Petrosian L., Olifan O., Kolomys O., Strelchuk V. Effect of magnesium doping on the structure, optical properties and photocatalytic efficiency of ZnO nanostructures deposited by atmospheric pressure MOCVD. *Chem. Phys. Lett.* 2024. **857**: 141720.
5. Chong M.N., Jin B., Chow C.W.K., Saint C. Recent developments in photocatalytic water treatment technology: A review. *Water Res*. 2010. **44**(10): 2997.
6. Lee K.M., Lai C.W., Ngai K.S., Juan J.C. Recent developments of zinc oxide based photocatalyst in water treatment technology: A review. *Water Res.* 2016. **88**: 428.
7. Kasumov A.M., Korotkov K.A., Karavaeva V.M., Zahornyi M.M., Dmitriev A.I., Ievtushenko A.I. Photocatalysis with the use of ZnO nanostructures as a method for the purification of aquatic environments from dyes. *J. Water Chem. Technol.* 2021. **43**(4): 281.
8. Sun Y., Zhang W., Li Q., Liu H., Wang X. Preparations and applications of zinc oxide based photocatalytic materials. *Adv. Sens. Energy Mater.* 2023. **2**(3): 100069.
9. Hamdam Momen M., Amadeh A., Heydarzadeh Sohi M., Moghanlou Y. Photocatalytic properties of ZnO nanostructures grown via a novel atmospheric pressure solution evaporation method. *Mater. Sci. Eng., B.* 2014. **190**: 66.
10. Fouad O.A., Ismail A.A., Zaki Z.I., Mohamed R.M. Zinc oxide thin films prepared by thermal evaporation deposition and its photocatalytic activity. *Appl. Catal. B Environ. Energy.* 2006. **62**(1–2): 144.
11. De Filpo G., Pantuso E., Armentano K., Formoso P., Di Profio G., Poerio T., Fontananova E., Meringolo C., Mashin A.I., Nicoletta F.P. Chemical Vapor Deposition of Photocatalyst Nanoparticles on PVDF Membranes for Advanced Oxidation Processes. *Membranes*. 2018. **8**(3): 35.
12. Maejima K., Fujita S. Chemical vapor reactions of ZnO growth by metal-organic vapor phase epitaxy. *J. Cryst. Growth.* 2006. **293**(2): 305.
13. Wang S.P., Shan C.X., Yao B., Li B.H., Zhang J.Y., Zhao D.X., Shen D.Z., Fan X.W. Electrical and optical properties of ZnO films grown by molecular beam epitaxy. *Appl. Surf. Sci*. 2009. **255**(9): 4913.
14. Gao W., Li Z. ZnO thin films produced by magnetron sputtering. *Ceram. Int.* 2004. **30**(7): 1155.
15. Baruah S., Dutta J. Hydrothermal growth of ZnO nanostructures. *Sci. Technol. Adv. Mater.* 2009. **10**(1): 013001.
16. Li H., Wang J., Liu H., Zhang H., Li X. Zinc oxide films prepared by sol–gel method. *J. Cryst. Growth.* 2005. **275**(1): 943.
17. Mukherjee N., Bhattacharyya P., Banerjee M., Mondal A., Gettens R., Ghosh P.K., Saha H. Galvanic deposition of nanocrystalline ZnO thin films from a ZnO–$Zn(OH)_2$ mixed-phase precursor on p-Si substrate. *Nanotechnology*. 2006. **17**(10): 2665.
18. Dedova T., Krunks M., Grossberg M., Volobujeva O., Oja-Acik I. A novel deposition method to grow ZnO nanorods: spray pyrolysis. *Superlattices Microstruct.* 2007. **42**(1–6): 444.
19. Li B., Liu T., Wang Y., Wang Z. ZnO/graphene-oxide nanocomposite with remarkably enhanced visible-light-driven photocatalytic performance. *J. Colloid Interface Sci.* 2012. **377**(1): 114.
20. Akir S., Hamdi A., Addad A., Coffinier Y., Boukherroub R., Omrani A.D. Facile synthesis of carbon–ZnO nanocomposite with enhanced visible light photocatalytic performance. *Appl. Surf. Sci.* 2017. **400**: 461.
21. Hamdam Momen M., Amadeh A., Heydarzadeh Sohi M., Moghanlou Y. Photocatalytic properties of ZnO nanostructures grown via a novel atmospheric pressure solution evaporation method. *Mater. Sci. Eng.: B*. **190**: 66.
22. Khranovskyy V., Lazorenko V., Lashkarev G., Yakimova R. Luminescence anisotropy of ZnO microrods. *J. Lumin.* 2012. **132**(10): 2643.
23. Weidenkaff A., Steinfeld A., Wokaun A., Auer P.O., Eichler B., Reller A. Direct solar thermal dissociation of zinc oxide: condensation and crystallisation of zinc in the presence of oxygen. *Solar Energy*. 1999. **65**(1): 59.
24. Ievtushenko A., Tkach V., Strelchuk V., Petrosian L., Kolomys O., Kutsay O., Garashchenko V., Olifan O., Korichev S., Lashkarev G., Khranovskyy V. Solar explosive evaporation growth of ZnO nanostructures. *Appl. Sci.* 2017. **7**: 383.
25. Mortezaali A., Moradi R. The correlation between the substrate temperature and morphological ZnO nanostructures for H_2S gas sensors. *Sens. Actuators, A*. 2014. **206**: 30.
26. Labhane P.K., Sonawane S.H., Sonawane G.H., Patil S.P., Huse V.R. Influence of Mg doping on ZnO nanoparticles decorated on graphene oxide (GO) crumpled paper like sheet and its high photo catalytic performance under sunlight. *J. Phys. Chem. Solids*. 2018. **114**: 71.
27. Taha K., Al Zoman M., Al Outeibi M., Alhussain S., Modwi A., Bagabas A.A. Green and sonogreen synthesis of zinc oxide nanoparticles for the photocatalytic degradation of methylene blue in water. *Nanotechnol. Environ. Eng.* 2019. **4**: 10.
28. Galdámez-Martinez A., Santana G., Güell F., Martínez-Alanis P.R., Dutt A. Photoluminescence of ZnO Nanowires: A Review. *Nanomaterials (Basel)*. 2020. **10**(5): 857.

29. Rasool A., Santhosh Kumar M.C., Mamat M.H., Gopalakrishnan C., Amiruddin R. Analysis on different detection mechanisms involved in ZnO-based photodetector and photodiodes. *J. Mater. Sci.: Mater. Electron.* 2020. **31**(9): 7100.
30. Pekar G.S., Singaevsky A.F., Kolomys O.F., Strelchuk V.V., Lytvyn P.M. Structural, optical and magnetic properties of stencil-free printed ZnO layers doped with Fe^{2+} and Fe^{3+} ions. *Mater. Chem. Phys*. 2022. **276**: 125329.
31. Taziwa R.T., Ntozakhe L., Meyer E. Structural, morphological and Raman scattering studies of carbon doped ZnO nanoparticles fabricated by PSP technique. *J. Nanosci. Nanotechnol.* 2017. **1**(1): 3.
32. Ievtushenko A., Karpyna V., Myroniuk L., Myroniuk D., Petrosian L., Olifan O., Kolomys O., Strelchuk V. Effect of magnesium doping on the structure, optical properties and photocatalytic efficiency of ZnO nanostructures deposited by atmospheric pressure MOCVD. *Chem. Phys. Lett.* 2024. **857**: 141720.
33. Mousa S.A., Wissa D.A., Hassan H.H., Ebnalwaled A.A., Khairy S.A. Enhanced photocatalytic activity of green synthesized zinc oxide nanoparticles using low-cost plant extracts. *Sci. Rep*. 2024. **14**: 16713.

Received 01.08.2025, accepted 25.02.2026